**Cell Reports, Volume *27***

## Supplemental Information

# An Intramolecular Salt Bridge Linking TDP43 RNA Binding, Protein Stability, and TDP43-Dependent Neurodegeneration

**Brittany N. Flores, Xingli Li, Ahmed M. Malik, Jose Martinez, Asim A. Beg, and Sami J. Barmada**

# Figure S1

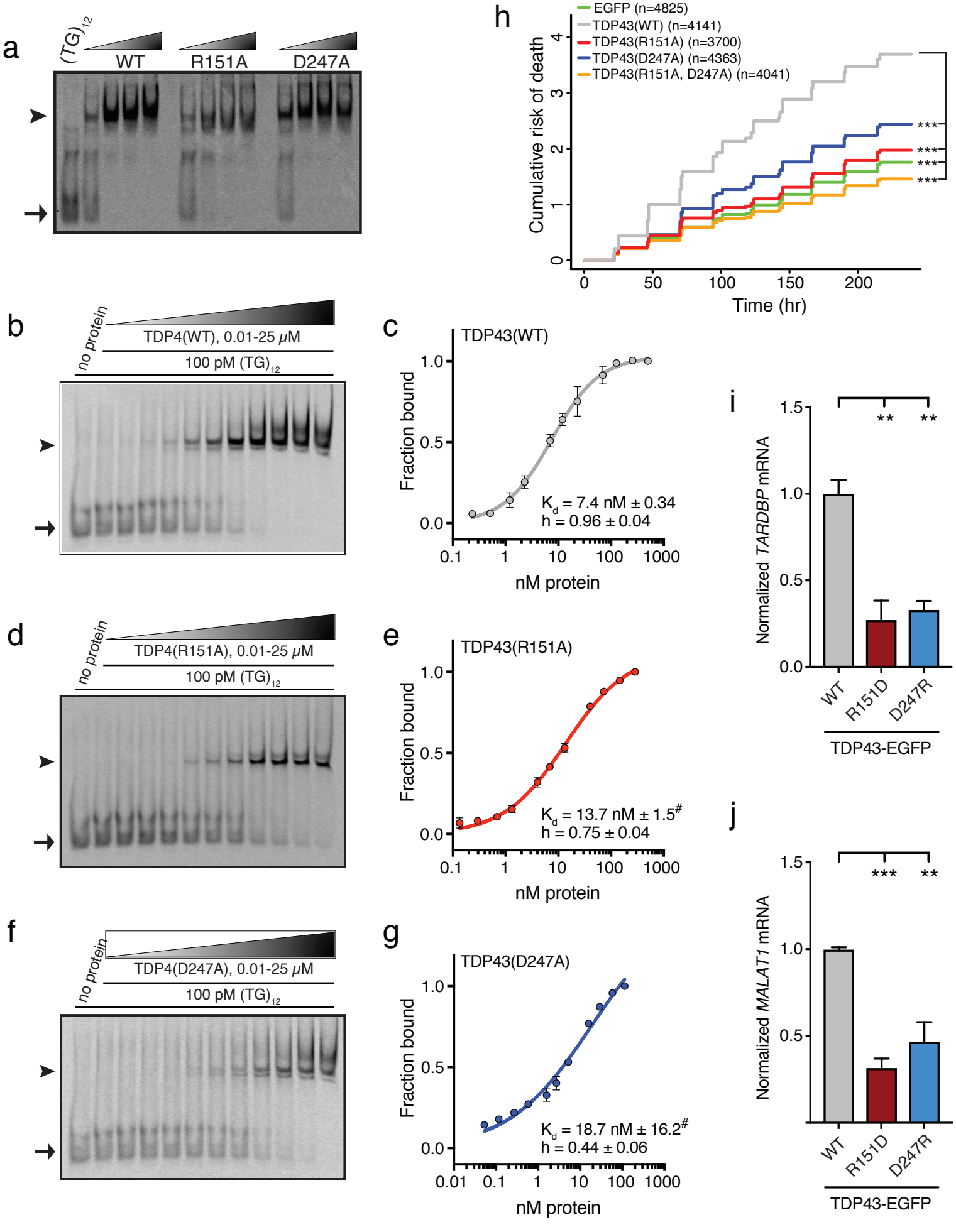
a
(TG)12
WT
R151A
D247A
b
no protein
TDP4(WT), 0.01-25 μM
100 pM (TG)12
c
TDP43(WT)
Fraction bound
Kd = 7.4 nM ± 0.34
h = 0.96 ± 0.04
nM protein
d
no protein
TDP4(R151A), 0.01-25 μM
100 pM (TG)12
e
TDP43(R151A)
Fraction bound
Kd = 13.7 nM ± 1.5#
h = 0.75 ± 0.04
nM protein
f
no protein
TDP4(D247A), 0.01-25 μM
100 pM (TG)12
g
TDP43(D247A)
Fraction bound
Kd = 18.7 nM ± 16.2#
h = 0.44 ± 0.06
nM protein
h
EGFP (n=4825)
TDP43(WT) (n=4141)
TDP43(R151A) (n=3700)
TDP43(D247A) (n=4363)
TDP43(R151A, D247A) (n=4041)
Cumulative risk of death
Time (hr)
i
Normalized TARDBP mRNA
WT
R151D
D247R
TDP43-EGFP
j
Normalized MALAT1 mRNA
WT
R151D
D247R
TDP43-EGFP

**Figure S1. Salt bridge disrupting mutations impair DNA binding by TDP43 and interfere with TDP43-dependent toxicity, related to Figures 1 and 5. a,** EMSA of recombinant TDP43 variants at increasing protein concentrations (12 fmol to 4 pmol) incubated with labeled $(TG)_{12}$ oligonucleotides (100 pM). **b, d, f,** Labeled $(TG)_{12}$ oligomers were added (100 pM) to increasing protein concentrations (0.01-25 μM). Three independent replicates for each protein were quantified in **c, e, g** to calculate dissociation constants ($K_d$) and Hill slopes. For **a**, **b, d, f,** arrowheads mark protein-DNA complexes, while arrows indicate free DNA oligomers. For **c, e,** and **g**, $K_d$ and Hill coefficient were determined by the nonlinear least squares regression fit equation, and each plot displays mean ± SEM; **#**, $p<0.01$ for comparison with TDP43(WT), extra sum-of-squares F test. **h**, Overexpressing TDP43(WT)-EGFP significantly enhances the cumulative risk of death compared to EGFP-expressing neuron (HR=2.43, $p<2x10^{-16}$) . Individual mutations that disrupt the salt bridge (R151A or D247A) significantly reduce toxicity compared to TDP43(WT)-expressing neurons (HR=0.47, and 0.58, respectively, $p<2x10^{-16}$ for both comparisons). Expression of TDP43(R151A, D247A)-EGFP significantly abrogates toxicity compared to TDP43(WT)-expressing neurons (HR=0.36, $p<2x10^{-16}$). n, number of neurons. *** $p<2x10^{-16}$, Cox proportional hazards. Survival analyses were collected from 3 independent experiments, with 8 wells per condition for each replicate. **i** and **j**, HEK293T cells were transfected with TDP43(WT), TDP43(R151D), or TDP43(D247R) and immunoprecipitated with antibodies against GFP. Bound *TARDBP* (**i**) or *MALAT1* (**j**) transcripts were amplified from total RNA by qRT-PCR. Data were pooled from 3 independent replicates. Plots show mean ± SEM, ** $p<0.05$, Kruskal-Wallis with Dunn's test.

# Figure S2

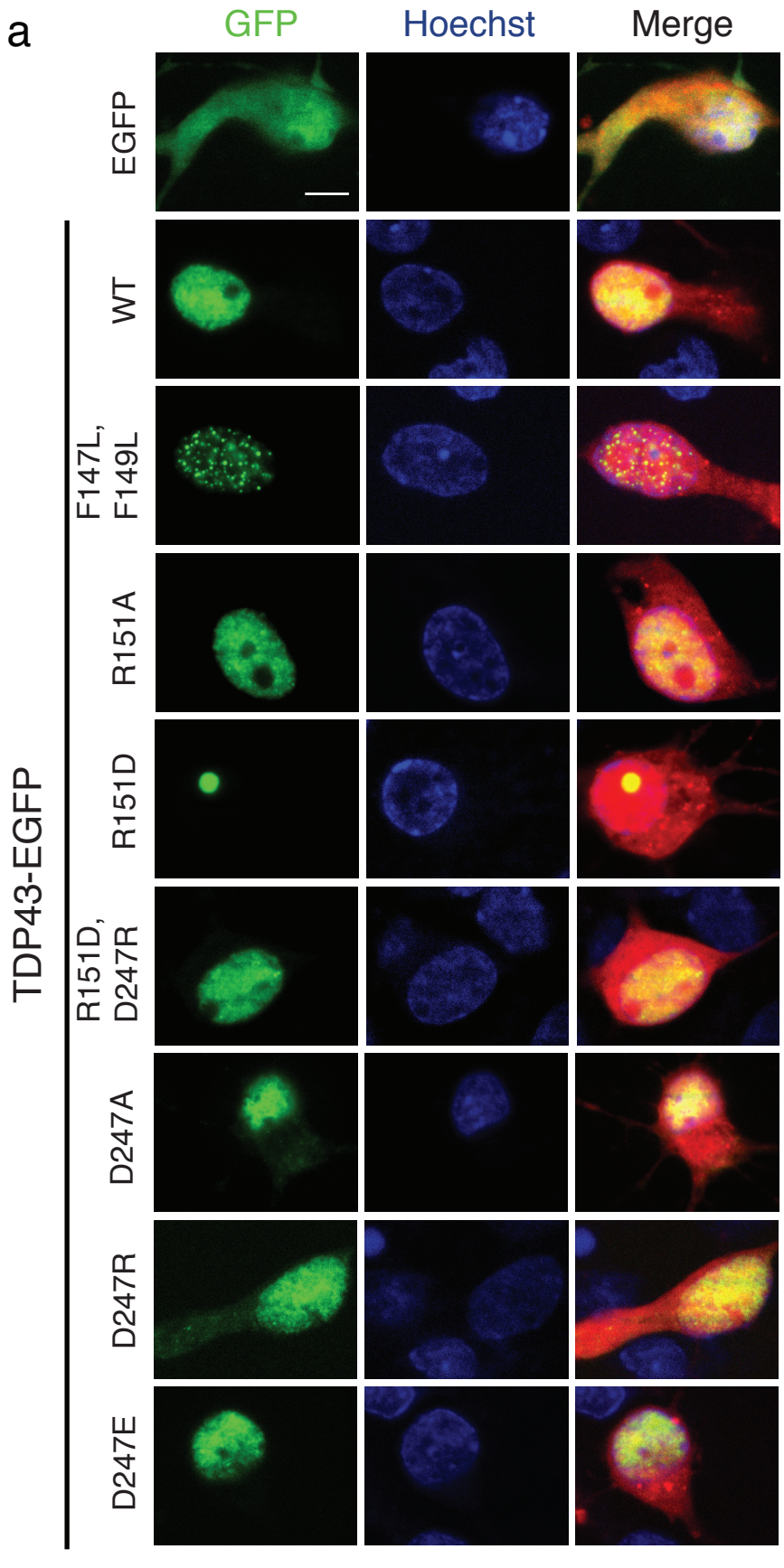
a
GFP
Hoechst
Merge
EGFP
TDP43-EGFP
WT
F147L, F149L
R151A
R151D
R151D, D247R
D247A
D247R
D247E

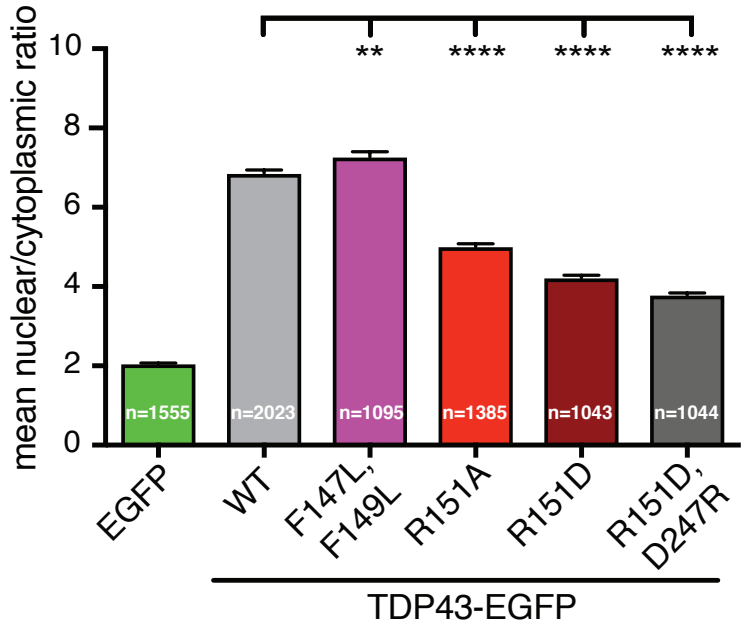
b
mean nuclear/cytoplasmic ratio
10
8
6
4
2
0
**
****
****
****
n=1555
n=2023
n=1095
n=1385
n=1043
n=1044
EGFP
WT
F147L, F149L
R151A
R151D
R151D, D247R
TDP43-EGFP

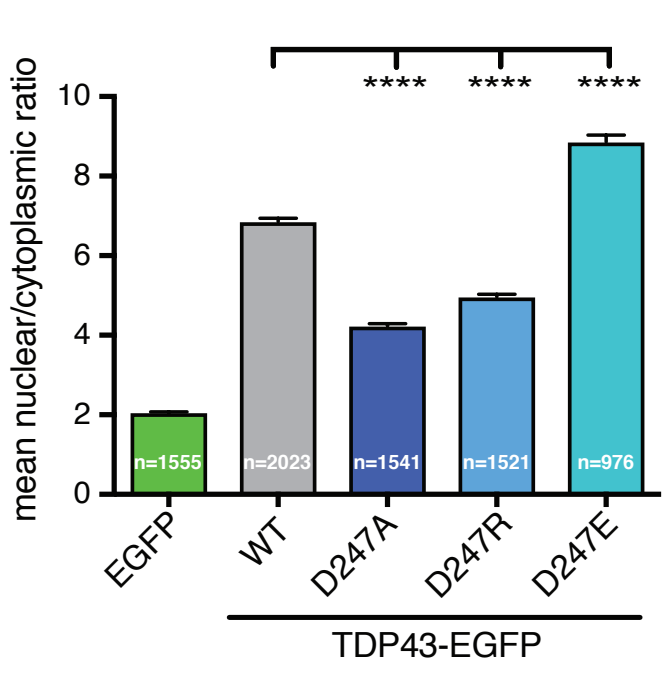
c
mean nuclear/cytoplasmic ratio
10
8
6
4
2
0
****
****
****
n=1555
n=2023
n=1541
n=1521
n=976
EGFP
WT
D247A
D247R
D247E
TDP43-EGFP

**Figure S2. Manipulating the RRM1-RRM2 salt bridge affects subcellular TDP43 localization, related to Figure 2. a,** Fluorescent microscopy of primary neurons expressing EGFP-tagged TDP43 variants. Nuclei were stained with a dye (4',6-diamidino-2-phenylindole (DAPI)). Scale bar: 5 μm. **b** and **c,** Subcellular TDP43-EGFP localization was quantified by measuring the fluorescence intensity of TDP43 within the nuclear and cytoplasmic compartments separately for each neuron. The mean nuclear-cytoplasmic ratio (NCR) for TDP43(WT) was 6.9±0.087. **b**, All variants of R151 significantly decreased the TDP43-EGFP NCR. **c**, Mutating D247 to either alanine or arginine decreased the NCR, while mutating D247 to glutamate significantly increased TDP43-EGFP NCR. Data in **b** and **c** represent at least 3 independent experiments, **** $p<0.0001$, one-way ANOVA with Dunnett's post-hoc. Plots in **b, c** show mean ± SEM; n, number of neurons.

# Figure S3

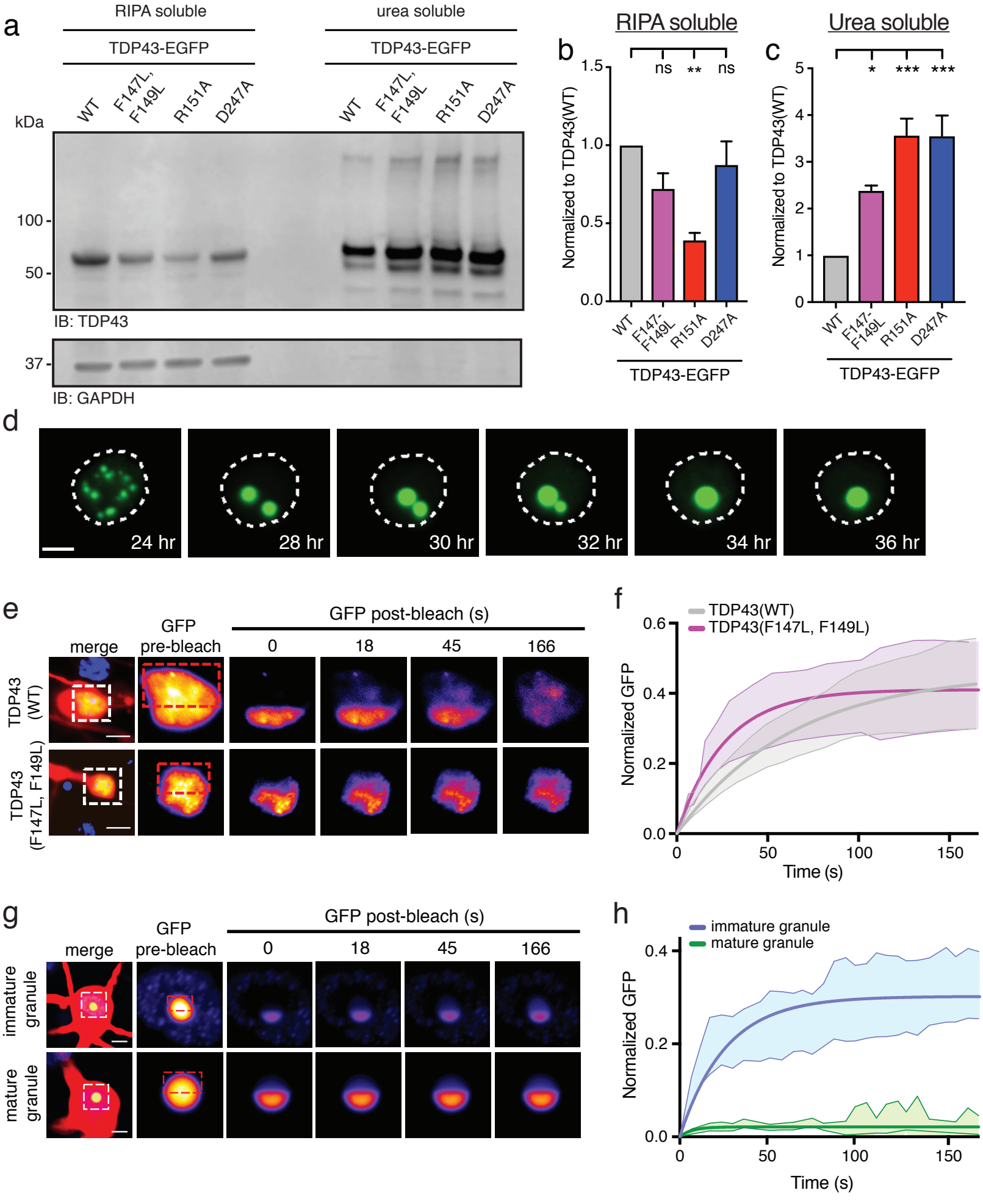
a
RIPA soluble
urea soluble
TDP43-EGFP
TDP43-EGFP
WT
F147L, F149L
R151A
D247A
WT
F147L, F149L
R151A
D247A
kDa
100
50
IB: TDP43
37
IB: GAPDH
b
RIPA soluble
ns
**
ns
Normalized to TDP43(WT)
1.5
1.0
0.5
0.0
WT
F147-F149L
R151A
D247A
TDP43-EGFP
c
Urea soluble
*
***
***
Normalized to TDP43(WT)
5
4
3
2
1
0
WT
F147-F149L
R151A
D247A
TDP43-EGFP
d
24 hr
28 hr
30 hr
32 hr
34 hr
36 hr
e
merge
GFP pre-bleach
GFP post-bleach (s)
0
18
45
166
TDP43 (WT)
TDP43 (F147L, F149L)
f
TDP43(WT)
TDP43(F147L, F149L)
Normalized GFP
0.6
0.4
0.2
0.0
0
50
100
150
Time (s)
g
merge
GFP pre-bleach
GFP post-bleach (s)
0
18
45
166
immature granule
mature granule
h
immature granule
mature granule
Normalized GFP
0.4
0.2
0.0
0
50
100
150
Time (s)

**Figure S3. Mutations that interfere with RNA binding reduce solubility and elicit liquid-liquid and liquid-gel phase transitions, related to Figure 2. a,** HEK293T cells were transfected with TDP43 variants, sonicated in RIPA buffer or extracted with urea buffer as indicated, and immunoblotted with anti-TDP43 antibodies. **b**, **c** Each TDP43 mutant was enriched within the urea-soluble fraction, compared to TDP43(WT). Data represent 3 independent replicates, *** $p<0.0001$, one-way ANOVA with Dunnett's post-hoc. Plots in **b**, **c** show mean ± SEM. **d,** TDP43(F147L, F149L)-EGFP shows time-dependent changes in distribution from diffuse to small puncta, which then fuse over time into large droplets consistent with liquid-like behavior. Scale bar: 5 μm. **e** and **f,** TDP43(F147L, F149L)-EGFP that has not phase separated and is still relatively diffuse in the nucleus shows no difference in its mobility compared to TDP43(WT)-EGFP (diffuse TDP43(WT) n = 4, diffuse TDP43(F147L, F149L) n = 5). **g** and **h,** Immature granules into which not all of the TDP43 has yet coalesced show internal rearrangement by fluorescence recovery after photobleaching (FRAP), consistent with liquid-liquid phase separated granules, but mature granules are nearly completely immobile (immature granules n = 3, mature granules n = 5). Scale bar: 10 μm. Data represent 3 independent replicates.

# Figure S4

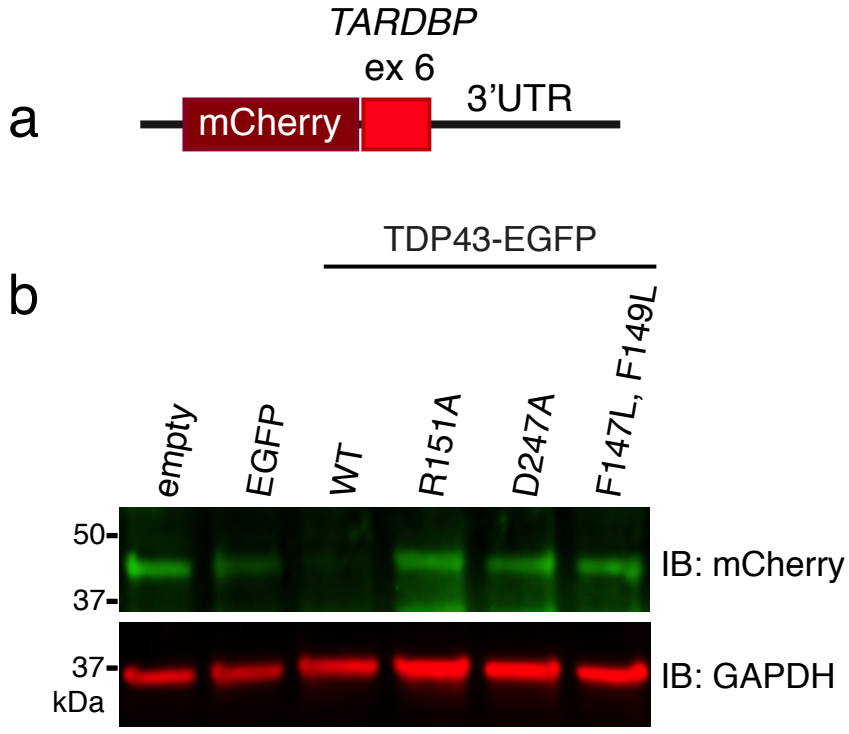
a
TARDBP
ex 6
mCherry
3'UTR
b
TDP43-EGFP
empty
EGFP
WT
R151A
D247A
F147L, F149L
50
37
IB: mCherry
37
kDa
IB: GAPDH

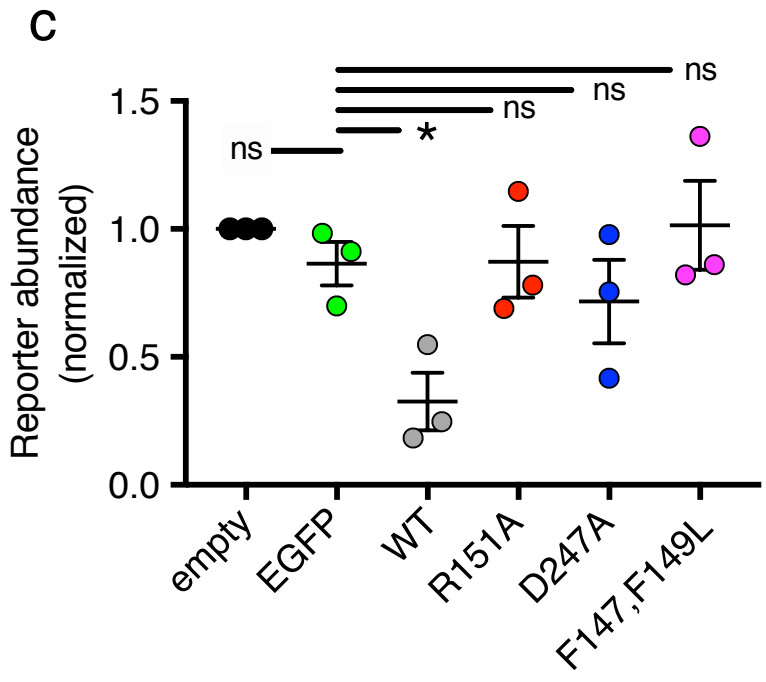
c
Reporter abundance
(normalized)
1.5
1.0
0.5
0.0
ns
*
ns
ns
ns
empty
EGFP
WT
R151A
D247A
F147,F149L

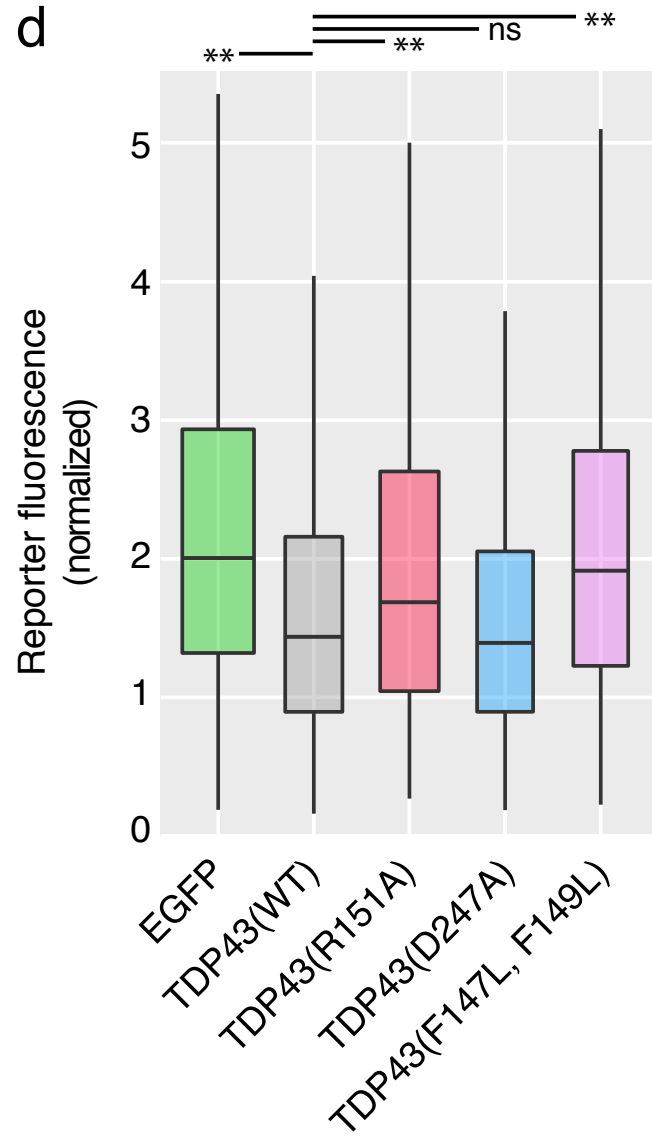
d
Reporter fluorescence
(normalized)
5
4
3
2
1
0
**
**
ns
**
EGFP
TDP43(WT)
TDP43(R151A)
TDP43(D247A)
TDP43(F147L, F149L)

**Figure S4. Salt bridge-disrupting mutations prevent TDP43 autoregulation, related to Figure 2. a**, Schematic illustration of a fluorescent TARDBP autoregulation reporter, consisting of mCherry located upstream *TARDBP* exon 6 and 3'UTR. **b**, HEK293T cells were co-transfected with the reporter and TDP43-EGFP variants, then immunoblotted with mCherry and GAPDH antibodies (**c**) or imaged by automated microscopy (**d**). Overexpression of TDP43(WT)-EGFP significantly reduced reporter abundance compared to EGFP in HEK293T cells (**c**) and primary neurons (**d**). Data represent 3 independent replicates, ** $p<0.001$, one-way ANOVA with Dunnett's post-hoc.

# Figure S5

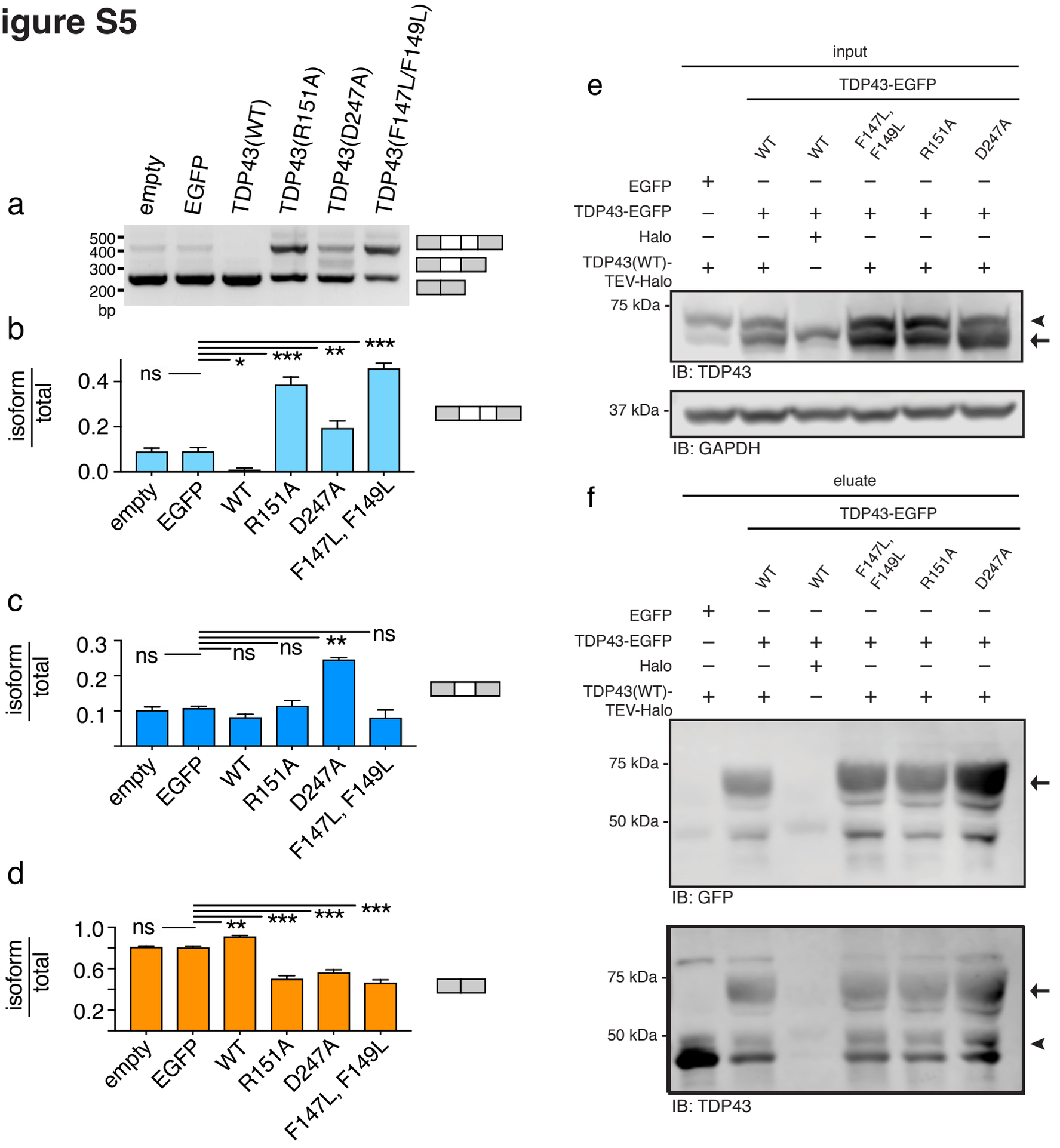
a
empty
EGFP
TDP43(WT)
TDP43(R151A)
TDP43(D247A)
TDP43(F147L/F149L)
500
400
300
200
bp
b
isoform / total
ns
*
***
**
***
0.4
0.2
0.0
empty
EGFP
WT
R151A
D247A
F147L, F149L
c
isoform / total
ns
ns
ns
**
ns
0.3
0.2
0.1
empty
EGFP
WT
R151A
D247A
F147L, F149L
d
isoform / total
ns
**
***
***
***
1.0
0.6
0.2
empty
EGFP
WT
R151A
D247A
F147L, F149L
e
input
TDP43-EGFP
WT
WT
F147L, F149L
R151A
D247A
EGFP + – – – – –
TDP43-EGFP – + + + + +
Halo – – + – – –
TDP43(WT)-TEV-Halo + + – + + +
75 kDa
IB: TDP43
37 kDa
IB: GAPDH
f
eluate
TDP43-EGFP
WT
WT
F147L, F149L
R151A
D247A
EGFP + – – – – –
TDP43-EGFP – + + + + +
Halo – – + – – –
TDP43(WT)-TEV-Halo + + – + + +
75 kDa
50 kDa
IB: GFP
75 kDa
50 kDa
IB: TDP43

**Figure S5. Overexpression of RNA binding-deficient TDP43 mutants impair TDP43-dependent splicing and physically interact with wild-type TDP43, related to Figure 2. a,** *CFTR* minigene splice products in HEK293 cells overexpressing EGFP or EGFP-tagged TDP43 variants. The top band represents exon 9 inclusion, the bottom band shows complete exon 9 exclusion, and the middle band arises from a cryptic splice event within exon 9. **b-d**, Quantification for each *CFTR* isoform. While TDP43(WT)-EGFP overexpression led to an increase in exon 9 exclusion, mutations disrupting RNA binding significantly decreased the proportion of transcripts with exon 9 exclusion. Data was pooled from 3 independent replicates, * $p<0.05$, ** $p < 0.01$, *** $p < 0.0001$; 2-way ANOVA with Dunnett's multiple comparison test. **e**, HEK293 cells co-expressing TDP43(WT)-HaloTag and EGFP-tagged TDP43(WT), TDP43(F147L, F149L), TDP43(R151A), or TDP43(D247A). Input samples were immunoblotted with anti-TDP43 and -GAPDH antibodies. **f**, HaloTag or TDP43(WT)-HaloTag was eluted with HaloLink, and eluates immunoblotted with anti-GFP and -TDP43 antibodies. TDP43(WT)-HaloTag associated with all TDP43-EGFP variants as detected by the ~75 kDa band corresponding to TDP43-EGFP in each lane. For **e** and **f**, arrow points to TDP43-EGFP. Arrowhead indicates TDP43-HaloTag for (**e**) and native TDP43 for (**f**). Immunoblots are representative of 3 biological replicates.

# Figure S6

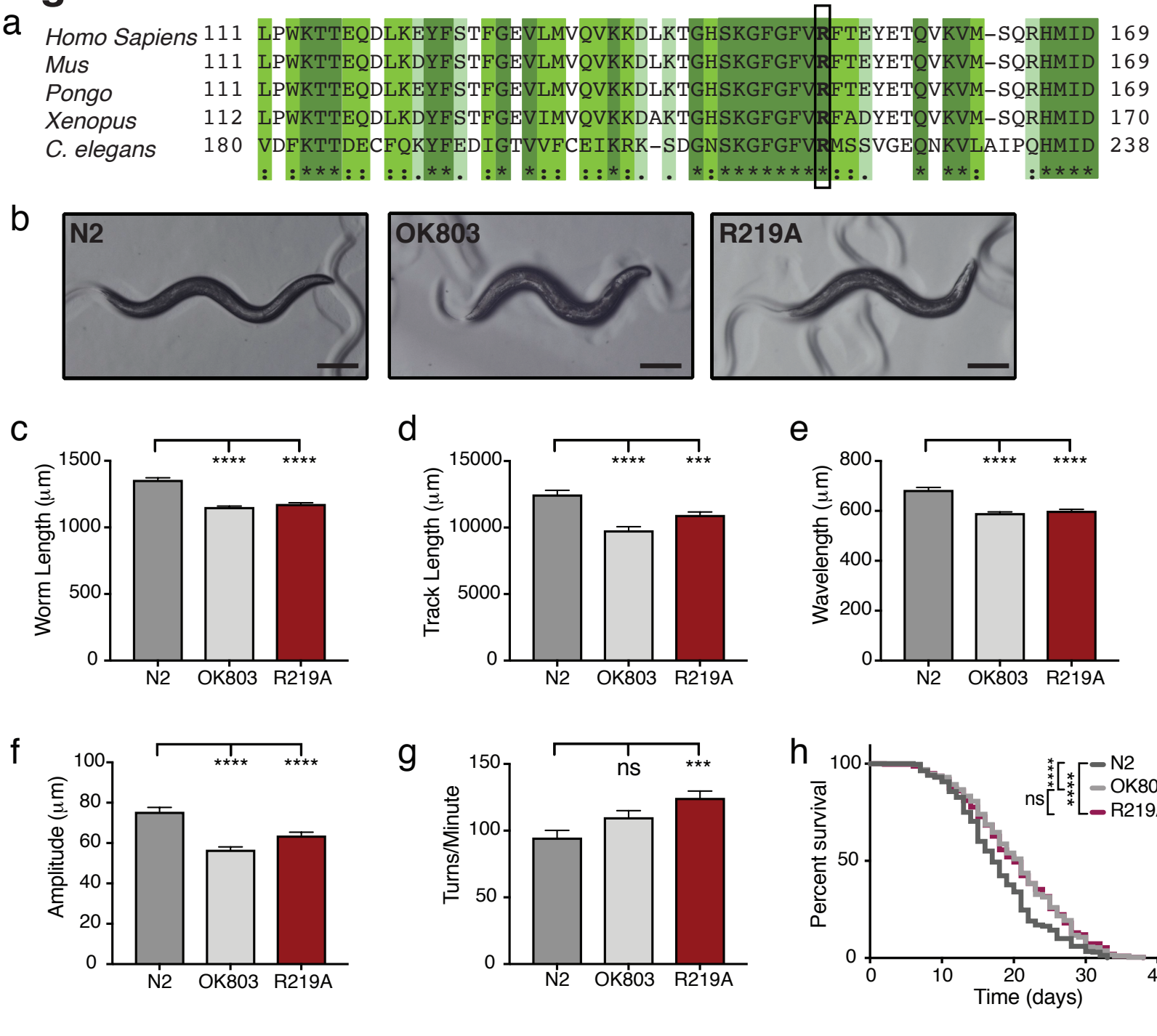
a
Homo Sapiens 111 LPWKTTEQDLKEYFSTFGEVLMVQVKKDLKTGHSKGFGFVRFTEYETQVKVM-SQRHMID 169
Mus 111 LPWKTTEQDLKDYFSTFGEVLMVQVKKDLKTGHSKGFGFVRFTEYETQVKVM-SQRHMID 169
Pongo 111 LPWKTTEQDLKEYFSTFGEVLMVQVKKDLKTGHSKGFGFVRFTEYETQVKVM-SQRHMID 169
Xenopus 112 LPWKTTEQDLKDYFSTFGEVIMVQVKKDAKTGHSKGFGFVRFADYETQVKVM-SQRHMID 170
C. elegans 180 VDFKTTDECFQKYFEDIGTVVFCEIKRK-SDGNSKGFGFVRMSSVGEQNKVLAIPQHMID 238
b
N2
OK803
R219A
c
Worm Length (µm)
1500
1000
500
0
****
****
N2
OK803
R219A
d
Track Length (µm)
15000
10000
5000
0
****
***
N2
OK803
R219A
e
Wavelength (µm)
800
600
400
200
0
****
****
N2
OK803
R219A
f
Amplitude (µm)
100
80
60
40
20
0
****
****
N2
OK803
R219A
g
Turns/Minute
150
100
50
0
ns
***
N2
OK803
R219A
h
Percent survival
100
50
0
0
10
20
30
40
Time (days)
ns
****
****
N2
OK803
R219A

**Figure S6. The *tdp-1*(R219A) knock-in phenocopies TDP-1 null mutations in *C. elegans*, related to Figure 2. a,** Interspecies sequence conservation of TDP43's RRM1 domain. Highly conserved residues are highlighted in green. Conservation of R151 (in bold) is highlighted. **b**, Representative images of 7d old wild-type (N2), *tdp-1 (ok803)* knockout, and mutant *tdp-1* (R219A) animals. Scale bar: 200 μm. **c-f,** Behavioral assays of 7d-old animals measuring worm length, track length, wavelength, and amplitude on NGM plates. Both *ok803* and R219A animals displayed significantly reduced locomotor metrics compared to N2 animals on NGM plates. **g,** Thrash assay measuring the number of body bends per minute in liquid media. R219A, but not *ok803,* animals displayed a significant increase in the number of body bends per minute compared to N2. **h**, An increase in survival was observed for both *ok803* and R219A animals compared to N2, but no significant difference was observed between *ok803* and R219A worms. **c**-**f**, data were pooled from 3 independent experiments, totaling $n \geq 127$ animals/genotype; **** $p<0.0001$, one-way ANOVA, Dunnett's post-hoc. **g**, data were pooled from 3 independent experiments, totaling $n \geq 96$ animals/genotype; **** $p<0.001$, one-way ANOVA, Dunnett's post-hoc. **h**, data were pooled from 3 replicates, totaling 418 animals/genotype; **** $p<0.0001$, log-rank test. Plots in **c**-**g** show mean ± SEM.

# Figure S7

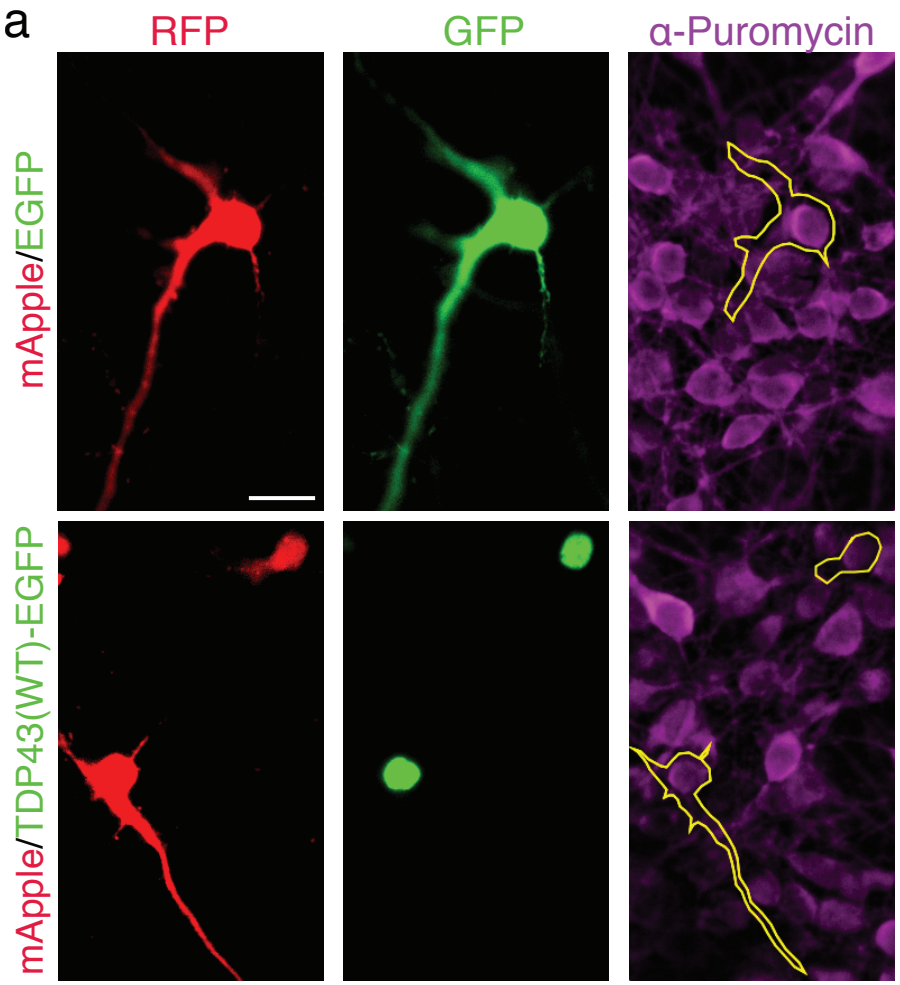
a
RFP
GFP
α-Puromycin
mApple/EGFP
mApple/TDP43(WT)-EGFP

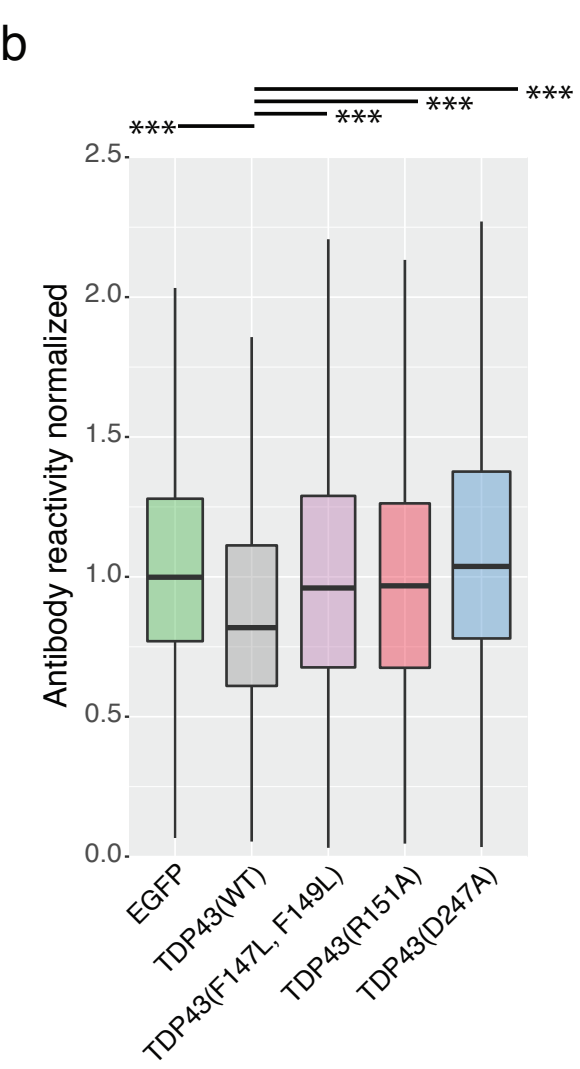
b
***
***
***
***
Antibody reactivity normalized
2.5
2.0
1.5
1.0
0.5
0.0
EGFP
TDP43(WT)
TDP43(F147L, F149L)
TDP43(R151A)
TDP43(D247A)

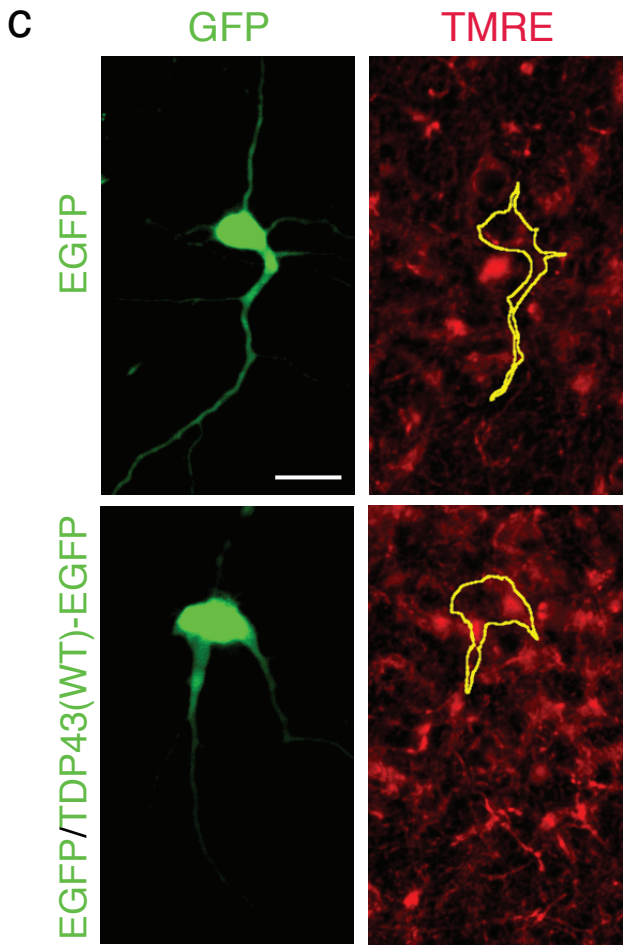
c
GFP
TMRE
EGFP
EGFP/TDP43(WT)-EGFP

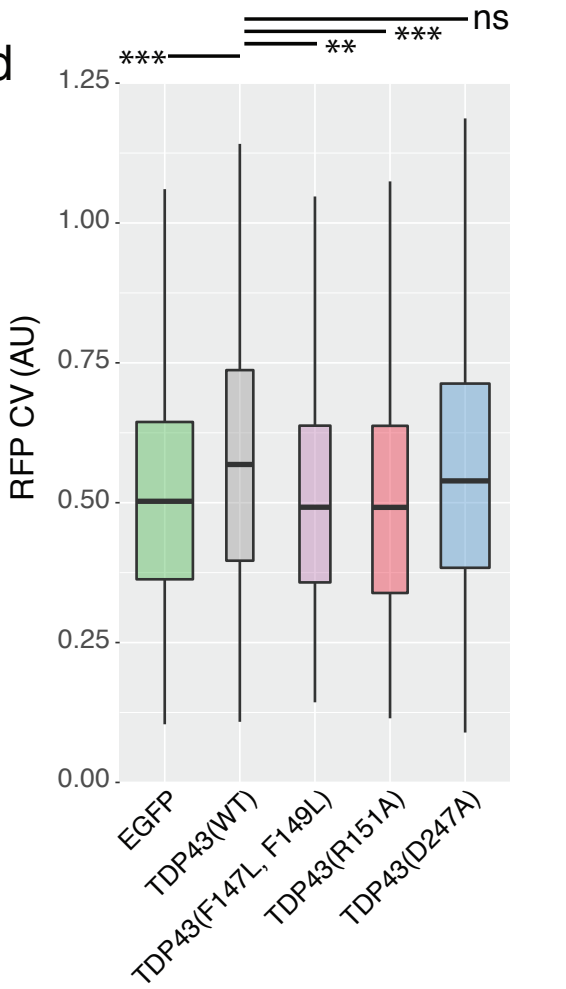
d
***
**
***
ns
RFP CV (AU)
1.25
1.00
0.75
0.50
0.25
0.00
EGFP
TDP43(WT)
TDP43(F147L, F149L)
TDP43(R151A)
TDP43(D247A)

**Figure S7. Protein synthesis and mitochondria morphology are altered in TDP43(WT)-expressing neurons, related to Figures 6 and 7. a,** Primary neurons were co-transfected with mApple and TDP43(WT)-EGFP or EGFP alone, treated with 1 μg/mL puromycin, and stained with puromycin antibodies. Yellow lines outline the cell bodies. **b**, TDP43(WT)-expressing neurons reduced protein synthesis by SUnSET. **c**, Fluorescent images of representative neurons overexpressing EGFP or TDP43(WT)-EGFP and EGFP and stained with the mitochondrial dye TMRE, demonstrating changes in mitochondria morphology in TDP43(WT)-expressing neurons. **d**, TDP43(WT)-EGFP and TDP43(D247A)-EGFP displayed elevated mitochondrial CV compared to EGFP. Data were collected from 2 independent experiments, ***p< 0.01, one-way ANOVA with Tukey's test. Scale bar: 20 μm.

**Table S1. Gene ontology of abnormally spliced transcripts, related to Figure 7.**

| KEGG Term | p | FE | Bonf. | Benj. | FDR | Genes |
|---|---|---|---|---|---|---|
| Ribosome | $6.6x10^{-17}$ | 3.0 | $3.1x10^{-14}$ | $3.1x10^{-14}$ | $1.4x10^{-13}$ | RPL18, RPL17, RPL19, RPL14, RPL13, RPS27L, RPS2, RPS3, RPLP0, RPLP1, RPL10, RPL11, RPL12, MRPL32, MRPL33, MRPL2, MRPL1, MRPL4, MRPL3, MRPS5, MRPL9, MRPS2, RPS18, RPS16, MRPS18A, RPS13, UBA52, MRPS17, MRPS16, MRPS11, MRPS10, RPS15A, RPL36, RPL37, MRPL10, RPS27, RPL30, RPS28, MRPL15, RPL32, RPL6, RPL31, RPL34, RPL9, RPL8, RPL3, RPL5, RPL7A, RPL10A, RPS24, RPSA, RPL26, RPL27, MRPS21, RPS6, RPS8, RPL28, RPS7, RPL23, RPL18A, RPL21, RPL37A |
| Spliceosome | $5.5x10^{-10}$ | 2.5 | $1.5x10^{-7}$ | $7.7x10^{-8}$ | $7.2x10^{-7}$ | HNRNPA1L2, NCBP1, CHERP, SRSF10, TRA2B, U2AF2, U2SURP, TRA2A, CWC15, SNU13, SF3B6, XAB2, SF3B4, SF3B2, HNRNPA3, HNRNPM, SF3B1, TCERG1, PLRG1, USP39, DHX15, MAGOHB, HNRNPC, ACIN1, RBM25, PRPF40A, RBM22, SNRPA1, ALYREF, SF3A2, DDX5, HNRNPA1, SF3A1, RBMX, HNRNPU, PRPF6, SRSF2, EIF4A3, PPIE, SRSF5, PPIH, SRSF6, SLU7, SNRNP40, SNRPC, PUF60, PRPF38B, THOC1, PRPF38A, SNRPG |
| Proteasome | $6.1x10^{-8}$ | 3.4 | $1.7x10^{-5}$ | $5.7x10^{-6}$ | $8.1x10^{-5}$ | PSMA7, PSMB5, PSMA1, PSMB4, PSMD14, PSMB7, PSMD13, PSMC5, PSMC4, PSMD11, PSMA5, PSMC3, PSME2, PSMA4, PSMC2, PSMA3, POMP, PSMD2, PSMD3, PSME3, PSME4, PSMD7, PSMD8 |
| Cell cycle | $1.5x10^{-7}$ | 2.3 | $4.3x10^{-5}$ | $1.1x10^{-5}$ | $2.0x10^{-4}$ | E2F3, FZR1, E2F4, PKMYT1, TTK, CHEK1, PTTG1, CDC16,ZBTB17, CDC45, ORC4, MYC, ORC1, CUL1, BUB3, TFDP1, STAG1, CDC7, CDK1, ANAPC2, ANAPC5, RBL1, ANAPC4, TP53, SKP2, MCM2, SKP1, MCM3, MCM4, CDC27, WEE1, CDC25A, MCM6, CDC25B, CCNB1, HDAC1, PLK1, PCNA, BUB1B, MDM2, ANAPC7, SMC1A, GADD45B |
| RNA transport | $8.6x10^{-7}$ | 2.0 | $2.4x10^{-4}$ | $4.9x10^{-5}$ | $1.1x10^{-3}$ | XPO1, NCBP1, RANGAP1, PNN, PRMT5, MAGOHB, NUP37, DDX20, ACIN1, TPR, TGS1, KPNB1, EIF2B4, EIF2B5, CLNS1A, NUP88, RAN, EIF2S3, NUP85, UBE2I, TACC3, EIF4G1, EIF4A3, EIF4G2, EIF4G3, AAAS, EIF4A2, EIF4A1, THOC6, NUP107, THOC1, NUP98, ELAC2, STRAP, PABPC4, NDC1, SUMO2, NUP214, EIF3B, EIF3G, EIF3E, NUP50, XPOT, GEMIN2, ALYREF, RNPS1, NXF1, CASC3, FXR1, EIF4B, SEC13, EIF4E2 |
| Base excision repair | $6.6x10^{-6}$ | 3.4 | $1.9x10^{-3}$ | $3.1x10^{-4}$ | $8.8x10^{-3}$ | APEX2, LIG1, NEIL3, POLE, NEIL1, MBD4, XRCC1, SMUG1, POLD4, MPG, MUTYH, POLE2, POLD1, POLD2, TDG, PCNA, PARP2 |
| DNA replication | $2.6x10^{-5}$ | 3.1 | $7.4x10^{-3}$ | $1.1x10^{-3}$ | $3.5x10^{-2}$ | LIG1, POLE, RNASEH1, POLA2, MCM2, MCM3, MCM4, RNASEH2C, MCM6, RFC5, POLD4, RFC1, POLE2, POLD1, PRIM2, POLD2,PCNA |

**Table S2. Primers used for site-directed mutagenesis, related to STAR methods.**

| Point Mutations or PCR Product | Amino Acid(s) | Primers | Sequences (5' – 3') |
|---|---|---|---|
| F147L/F149L | 147,149 | Forward | GGT CAT TCA AAG GGG CTT GGC CTT GTT CGT TTT ACG G |
| | | Reverse | CCG TAA AAC GAA CAA GGC CAA GCC CCT TTG AAT GAC C |
| R151A | 151 | Forward | GGT TTG GCT TTG TTG CTT TTA CGG AAT ATG |
| | | Reverse | CAT ATT CCG TAA AAG CAA CAA AGC CAA ACC |
| R151D | 151 | Forward | GGG GTT TGG CTT TGT TGA TTT TAC GGA ATA TG |
| | | Reverse | CAT ATT CCG TAA AAT CAA CAA AGC CAA ACC CC |
| D247A | 247 | Forward | CTC TTT GTG GAG AGG CCT TGA TCA TTA AAG G |
| | | Reverse | CCT TTA ATG ATC AAG GCC TCT CCA CAA AGA G |
| D247R | 247 | Forward | CTC TTT GTG GAG AGC GCT TGA TCA TTA AAG |
| | | Reverse | CTT TAA TGA TCA AGC GCT CTC CAC AAA GAG |
| D247E | 247 | Forward | GTC TCT TTG TGG AGA GGA GTT GAT CAT TAA AGG AAT C |
| | | Reverse | GAT TCC TTT AAT GAT CAA CTC CTC TCC ACA AAG AGA C |
| mPUM2 | 255, 256, 259 | Forward | CAC AAA TTT GCC GCC GCT GTA GTA GCA AAG TGT GTT ACT C |
| | | Reverse | GAG TAA CAC ACT TTG CTA CTA CAG CGG CGG CAA ATT TGT G |
| PP7 | 1-283 | Forward | TCC AAA ACC ATC GTT CTT TCG G |
| | | Reverse | TCC TCC TCC GCT TCC TCC ACT A |
| TDP43 N-terminus | 1-106 | Forward | ATG TCT GAA TAT ATT CGG GTA ACC G |
| | | Reverse | TAA ATC GGA TGT TTT CTG GAC T |
| TDP43 C-terminus | 263-414 | Forward | AAG CAC AAT AGC AAT AGA CAG TTA G |
| | | Reverse | TCC CCA GCC AGA AGA CTT AGA ATC C |
| TDP43(RRM1) | 107-176 | Forward | ATA GTG TTG GGT CTC CCA T |
| | | Reverse | GCT TCT CAA AGG CTC ATC TT |
| TDP43(RRM2) | 191-262 | Forward | CTT CCT AAT TCT AAG CAA AGC CAA G -3' |
| | | Reverse | AGG TTC GGC ATT GGA TAT ATG AAC GC – 3 |
| TDP43(WT) | 1-414 | Forward | GCT AGC GCC ACC ATG TCT GAA TAT ATT |
| | | Reverse | ACC GGT CCC AAA CCT CTA CCG TCC CA |
| HaloTag | 1-296 | Forward | ATG GCA GAA ATC GGT ACT GG |
| | | Reverse | CTA GGA AAT CTC GAG CGT CGA CA |
| TEV | 1-7 | Forward | GAG AAT CTT TAT TTT CAG GGC |
| | | Reverse | GCC CTG AAA ATA AAG ATT CTC |

**Table S3. Additional oligonucleotides, related to STAR methods.**

| Oligonucleotide | Source | Sequences (5' – 3') | |
|---|---|---|---|
| Dendra2-CL1 gene block | IDT | ACC GGT TGC CAC CAT GAA CAC CCC GGG AAT TAA CCT GAT CAA GGA GGA CAT GCG CGT GAA GGT GCA CAT GGA GGG CAA CGT GAA CGG CCA CGC CTT CGT GAT CGA GGG CGA GGG CAA GGG CAA GCC CTA CGA GGG CAC CCA GAC CGC CAA CCT GAC CGT GAA GGA GGG CGC CCC CCT GCC CTT CAG CTA CGA CAT CCT GAC CAC CGC CGT GCA CTA CGG CAA CCG GGT GTT CAC CAA GTA CCC CGA GGA CAT CCC CGA CTA CTT CAA GCA GAG CTT CCC CGA GGG CTA CAG CTG GGA GCG CAC CAT GAC CTT CGA GGA CAA GGG CAT CTG CAC CAT CCG CAG CGA CAT CAG CCT GGA GGG CGA CTG CTT CTT CCA GAA CGT GCG CTT CAA GGG CAC CAA CTT CCC CCC CAA CGG CCC CGT GAT GCA GAA GAA GAC CCT GAA GTG GGA GCC CAG CAC CGA GAA GCT GCA CGT GCG CGA CGG CCT GCT GGT GGG CAA CAT CAA CAT GGC CCT GCT GCT GGA GGG CGG CGG CCA CTA CCT GTG CGA CTT CAA GAC CAC CTA CAA GGC CAA GAA GGT GGT GCA GCT GCC CGA CGC CCA CTT CGT GGA CCA CCG CAT CGA GAT CCT GGG CAA CGA CAG CGA CTA CAA CAA GGT GAA GCT GTA CGA GCA CGC CGT GGC CCG CTA CAG CCC CCT GCC CAG CCA GGT GTG GGC ATG CAA GAA CTG GTT CTC TAG CCT GTC CCA CTT CGT CAT CCA TCT GTA AGT CGA C (CL1 sequence underlined) | |
| $(UG)_{12}$ | IDT | 5IRD800CWN-UGUGUGUGUGUGUGUGUGUGUG | |
| $(TG)_{12}$ | IDT | 5IRD700-TGTGTGTGTGTGTGTGTGTGTGTG | |
| $(AT)_{12}$ | IDT | 5IRD700-ATATATATATATATATATATATAT | |
| $(GC)_{12}$ | IDT | 5IRD700-GCGCGCGCGCGCGCGCGCGCGC | |
| qPCR primers for *TARDBP* | IDT | Forward | GTGGCTCTAATTCTGGTGCAG |
| | | Reverse | CACAACCCCACTGTCTACATT |
| qPCR primers for *MALAT1* | IDT | Forward | GACGGAGGTTGAGATGAAGC |
| | | Reverse | ATTCGGGGCTCTGTAGTCCT |